

Wind farm array cable layout optimisation for complex offshore sites—A decomposition based heuristic approach

Peter Taylor¹  | Hong Yue² | David Campos-Gaona² | Olimpo Anaya-Lara² | Chunjiang Jia³

¹EPSRC Doctoral Training Centre for Wind and Marine Energy Systems, University of Strathclyde, Glasgow, UK

²Wind Energy and Control Centre, Department of Electronic and Electrical Engineering, University of Strathclyde, Glasgow, UK

³Offshore Renewable Energy Catapult, Offshore House, Albert Street, Blyth, UK

Funding information

Engineering and Physical Sciences Research Council, Grant/Award Number: EP/L016680/1

Abstract

As the number of turbines in offshore wind farms increases, so does the complexity of cable routing optimisation problems. Optimising the collector network is a crucial task for developers contributing between 15% and 30% of initial investment costs. For some algorithms, increasing the number of turbines leads to unfavourable scaling of the computational time and memory required to reach optimal solutions. Heuristics offer an alternative but are likely to incur increases in total costs relative to the optimal solution since heuristic searching cannot guarantee optimality. This study proposes a novel optimisation algorithm based on the ant-colony heuristic by introducing decomposition techniques informed by the problem formulation to improve the computational performance. The new algorithm can reach near-optimal solutions and requires little computational resource. Three algorithms are compared on a set of six case studies, including mixed-integer linear programming (MILP), classical ant-colony optimisation (ACO) algorithm, and the proposed ACO with decomposition, ACOsp. Optimal solutions were found using the MILP algorithm. ACO algorithm solutions cost 0.4–7.6% more than optimal solutions, whereas ACOsp solutions cost only 0.0–1.4% more than optimal solutions. The proposed ACOsp algorithm has shown to be a robust approach for large-scale cable layout optimisation problems (>100 turbines) without requiring high-performance computing facilities.

1 | INTRODUCTION

The electrical infrastructure of offshore wind farms contributes a very large capital cost to projects, at approximately 15–30% of the total initial investment costs [1, 2]. Additionally, since most of this infrastructure is sub-sea, it is more difficult and expensive to access than in an onshore wind farm, with access far more subject to weather conditions and favourable sea states. This high cost and difficult access make the electrical infrastructure an excellent candidate for optimisation algorithms to find the optimal layout solution and minimise the total network length, capital costs, and associated electrical losses.

1.1 | Collector network topologies and attributes

Various recent studies, particularly since 2010, have investigated collector network topologies to reduce the cost of the array

cables through cost comparisons, modelling, and redundancy measures. A chosen topology heavily influences the electrical losses of the cable network, however has little impact on the voltage levels throughout the collector system [3]. Detailed cost modelling of the system, and the different topologies, is necessary to accurately assess the quality of proposed layouts, which can have significant impacts on decisions such as whether or not a substation is required. For example, one study, considering a small 150MW wind farm, showed that a substation was necessary only when the wind farm was further than 3 km from the shore [4]. Reliability assessments and consideration of strategically placed breakers and redundant cables have been shown to improve solutions, when compared to real wind farm sites such as the Lillgrund offshore wind farm [3, 5]. Real projects typically use multiple cable sizes, which is an important factor influencing the cost, so selecting the most suitable cable rating for each section is essential for the whole infrastructure optimisation. While most approaches identify the peak current of a given connection and size the cables accordingly, it has been shown that

This is an open access article under the terms of the [Creative Commons Attribution](https://creativecommons.org/licenses/by/4.0/) License, which permits use, distribution and reproduction in any medium, provided the original work is properly cited.

© 2022 The Authors. *IET Renewable Power Generation* published by John Wiley & Sons Ltd on behalf of The Institution of Engineering and Technology.

considering equivalent cyclical loading and temperature limits of cables can greatly reduce the necessary cable rating. One such study demonstrated that only two of the original three export cables were necessary for a real site case study, however, noted that lost revenue may need to be taken into account during long periods of high wind speeds [6]. Larger cables tend to be favoured in routing and optimisation studies that consider lifetime costs and electrical losses, compared to real world networks [7, 8]. However, the trend of increasing cable ratings to reduce the electrical losses has been shown to be a valid strategy with limitations. One study demonstrated that sizing cables to carry the total power of a string and the total power of a neighbouring string—during a fault, through a redundant connection—was not cost effective [8].

1.2 | Optimisation: Mixed-integer linear programming (MILP)

MILP and similar methods have been the focus of many studies investigating wind farm collector network layout optimisation, where a combination of binary and non-binary variables are employed to describe the location and size of cables [9]. Studies taking this approach have shown that branched layouts outperform non-branched radial layouts and that using offshore transformer modules at selected turbines instead of a dedicated substation can greatly reduce lifetime costs [10]. The MILP formulation is also capable of considering looped cable layouts and branching connection costs [11, 12], as well as utilising Steiner (non-turbine or empty) nodes for obstacle avoidance [1]. MILP can be used to solve problems of a capacitated minimum spanning tree formulation and has been used in conjunction with path-finding algorithms, substation positioning [13], and turbine layout optimisation [14]. The MILP method though, can be very computationally expensive, particularly in terms of its memory requirements. This means the algorithm is not a sufficient solver for large problems and may need ‘warm-starting’ by providing a reasonable starting solution [15]. For example, one study optimised sub-problems of a larger cable layout problem, to seed the final MILP solver with a sufficiently good quality initial solution [1]. Using this method, the solver was able to find the optimal solution to approximately half of the case study scenarios within 24 h. Furthermore, an earlier integer linear programming (ILP) study employed a cutting-planes method to improve the performance of its ILP solver, but suggested that heuristics may be a good approach for Steiner tree problems such as offshore wind farm cable layout optimisation [16]. A more recent ILP study considered wind farms with several substations and allowed connections to another local wind farm. The largest case study considered contained 102 turbines and generated solutions quickly, but lacked several key constraints such as the wind farm boundary, obstacle regions, and cable crossing constraints [17].

1.3 | Optimisation: Heuristic algorithms

Other approaches have been taken in the cable layout optimisation literature, with heuristics offering a good alternative to MILP-based solvers. Heuristics, although not guaranteed to find the optimal solution, have been shown to produce good quality solutions. One study on a no-branching layout demonstrates that the cost of the heuristic designed layouts is only 2% more than the global optimal solution [18]. Another study demonstrated that a Voronoi diagram based adaptive particle swarm optimisation method with additional local search heuristic could produce a 12.74% cost reduction compared to a benchmark case [19]. Clustering-based algorithms, such as quality threshold (QT) clustering, optimise solutions that reduce electrical losses and improve reliability, but increase the capital expenditure. These QT algorithms, despite generating good quality solutions, can lead to a high degree of cable connections at turbines, with one study’s proposed layout having 13 cables entering a turbine node [20] which is not a feasible solution in reality. Similar approaches have been taken focusing on optimising the grouping of turbines to be connected in strings, for example, grouping turbines using k-means clustering and a genetic algorithm (GA), while relying on a simple minimum spanning tree (MST) algorithm to compute the shortest cable routing for each group [21]. Similarly, a Euclidean minimum Steiner tree approach has been explored, utilising a ‘GeoSteiner’ algorithm solver. This method was able to generate solutions to small problems (approx. 30 turbines) in less than 1 h, however the computational time quickly increased to around 10 h for larger cases (approx. 50 turbines). Additionally, the proposed layout solutions contained many branching connections at the Steiner nodes, which again is not a practical solution for real offshore cases [22]. Other heuristic methods have been shown to be computationally fast with one study utilising a large neighbourhood search algorithm, followed by swapping and re-partitioning heuristics, claiming two orders of magnitude reduction in time-to-solutions [23]. GAs are promising heuristic methods, capable of handling large numbers of turbines to connect through the collector network, with one study considering 280 turbines [24]. GAs are not without limitations, however, and it is important to ensure the parameters are well tuned to the problem under consideration. For example, in the mentioned case of 280 turbines, the resulting solution contained many crossing cables, one string that was not connected to a substation, and a few strings that could be seen through visual inspection to be non-optimal [24]. Combining a GA approach with clustering techniques and Clark and Wright’s saving algorithm was shown to provide consistent and economically efficient layout solutions [25].

1.4 | Electrical losses

As mentioned previously, the layout topology heavily influences electrical losses of the system, and vice versa [3, 26]. Therefore,

most studies in the literature include electrical losses as a key component of their objective function. Some studies simplify this calculation to limit the impact on computational time, for example by assuming that the current experienced by a cable is half of the current at rated power [27]. This proxy for the true current profile of a cable connection may be computationally quicker, but introduces significant assumptions about the non-linear electrical losses of the cables. Typically, studies that compute electrical losses for cables do so in a pre-optimisation phase, where losses are calculated for each cable under different scenarios (supporting different numbers of turbines) [9, 28]. The losses then can be appropriately considered for each cable in a given layout, considering the losses for the correct scenario/electrical-loading. Since the cost of electrical losses is a function of the price of energy, some consideration has been given to the effect of a changing price of energy in the future. It has been shown that, for a realistic fluctuation in the energy price, the optimal layout of the collector network was not significantly affected [28].

1.5 | Ant-colony optimisation (ACO)

The ACO algorithm was introduced in 1999 as a common framework for the many ant-system algorithms of the time [29], presenting applications of the algorithm to travelling salesman problems (TSP) and network routing problems. ACO has only been used in a few cable routing optimisation studies, one of which generated a cable layout solution that is clearly non-optimal by visual inspection [30]. As a heuristic approach, it is important to ensure that the parameters are reasonably tuned for the problem. Other possible errors may be recording the solution of the final iteration rather than the 'global best' solution. ACO has been demonstrated on cases containing 280 turbines [31], optimising cable routing for different substation positions. While this scale of problem is more in-line with modern wind farm sizes, the study restricted the algorithm to one type of cable, therefore no cable selection algorithm was necessary.

1.6 | Decomposition strategies

As modern wind farms increase in size - both in terms of power generation and the number of turbines—the complexity of cable layout problems increases dramatically, and even more so for integrated optimisation of cable and turbine layouts [32]. It is also increasingly important to optimise the cable layout, rather than restrict it to any given topology in advance [32]. Therefore, cable layout optimisation algorithms must be robust and computationally efficient, a challenging issue for which decomposition strategies may be able to provide a solution. Many optimisation algorithms use branch-and-bound (B&B) techniques within the solver. Hendrix et al (2010 pg.159) highlighted the similarity of this process to problem decomposition

as “The basic idea in B&B methods consists of a recursive decomposition of the original problem into smaller disjoint sub-problems until the solution is found” [33]. The decomposition of a problem can be considered as the isolation of a subset of the decision variables for optimisation, while all other variables remain fixed. Recursively decomposing a problem into different subsets of the decision variables allows solvers to reach optimal solutions more quickly. Several studies have employed decomposition techniques (beyond the B&B algorithm in solvers) to improve the performance of their MILP algorithms [34], in some cases reducing computational time by up to 98% [35].

Considering existing approaches, there is a lack of robust and computationally efficient algorithms for large-scale array cable layout optimisation problems that generate solutions at, or close to, optimality. This study investigates how a suitable decomposition strategy may be integrated with an ACO algorithm for cable layout optimisation of a large offshore wind farm. Unlike some other simple turbine clustering techniques, the proposed decomposition strategy is informed by the problem formulation (i.e. that cables are connected in strings) to recursively create a subsets of the decision variables for optimisation. This approach aims to provide the benefits in computational speed from heuristic methods while finding the optimal (or near optimal) solutions that integer linear programming methods are able to generate. A comparison is made between the widely used MILP algorithm, a classical ACO algorithm, and an ACO algorithm making use of a simple decomposition strategy. The remainder of the paper includes the following: Section 2 presents the three optimisation algorithms for comparison; Section 3 introduces the case study of the hypothetical large offshore wind farm; Section 4 gives results and discussion on the effectiveness of the three approaches, including consideration of constraints to avoid crossing cables; and Section 5 presents the conclusions and future work. A full set of results and the coordinates of the case study turbine positions are provided in the Appendix.

2 | OPTIMISATION METHODS

This section outlines the three optimisation algorithms for comparison: MILP, ACO and ACO with decomposition into sub-problems (hereafter referred to as ACOsp). Common to all three methods is a pre-processing phase considering problem formulation, electrical loss calculation, and creation of the available cable set. The objective function and specific constraints used in each algorithm are elaborated in the following sections. The goal of all three algorithms is to find a cable layout that connects all turbines to a substation for the generated power to be exported. Turbines may be connected in strings and branched connections are allowed in the solutions. The cable sizes selected for each cable connection must also be capable of carrying the rated power of the number of turbines it is supporting. Only one cable may leave each turbine and any crossing sections incur a penalty cost in the objective value.

TABLE 1 Example set of cable types (conductor sizes under different electrical loading scenarios), with the associated costs and net present value (NPV) of electrical losses. (Representative values generated by the authors)

Cable conductor size (mm ²)	No. turbines supported	Capital cost (£/m)	Electrical losses (NPV, £/m)	Total cost (£/m)
95	1	120	20	140
95	2	120	40	160
95	3	120	75	195
180	1	150	10	160
180	2	150	20	170
180	3	150	40	190
180	4	150	80	230
240	1	175	5	180
240	2	175	10	185
240	3	175	20	195
240	4	175	40	215
240	5	175	75	250

2.1 | Pre-processing

In order to define the problem for optimisation, the coordinates of the wind farm boundary, obstacles, and turbines are required in addition to the cable parameters. A description of the wind field and turbine performance curves are also necessary for the calculation of electrical losses.

For each of the available cable sizes, a subset of cables is created considering different electrical loading scenarios (different numbers of turbines being supported). The net present value (NPV) of the electrical losses is calculated as follows for each of the available cables, under each of the loading scenarios.

$$loss_n^t = 8760 I_n^2 R^t k_{MWh} \sum_{yr=0}^{LT} \frac{1}{(1+d)^{yr}} \quad (1)$$

where $loss_n^t$ is the NPV electrical losses for a cable of type t supporting n turbines, I_n is the current profile in an arc supporting n turbines, R^t is the resistance per unit length of cable type t , k_{MWh} is the price per MWh, LT is the project lifetime in years, and d ($0 < d < 1$) is the discount rate. An example set of representative cables and their associated costs are shown in Table 1 (representative values generated by the authors for the purpose of demonstration).

In order to reduce the complexity of the problem and improve performance of the algorithm, the set of available cables can be reduced, simplifying the cable selection process. In the algorithms in the following sections, the cable routing and cable sizes must be determined. Cables will be supporting a given number of turbines for each connection and it is important that the cheapest overall cable is chosen (whilst obeying capacity constraints). Table 2 shows a reduced subset of cables,

TABLE 2 Example of a reduced set of cables with associated costs, from the larger set of cables presented in Table 1, keeping only the cheapest cable per number of turbines to be supported

Cable conductor size (mm ²)	No. turbines supported	Capital cost (£/m)	Electrical losses (NPV, £/m)	Total cost (£/m)
95	1	120	20	140
95	2	120	40	160
180	3	150	40	190
240	4	175	40	215
240	5	175	75	250

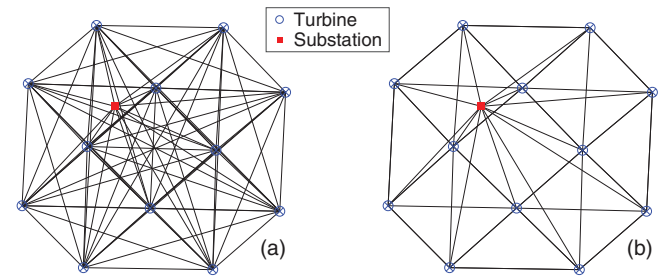


FIGURE 1 Example case of 12 turbines and 1 substation, with (a) all possible cable connections and (b) cable connections limited from each turbine to the nearest 4 turbines and the substation

keeping only the cheapest cable (by total cost) for each number of turbines to be supported. For example, each of the three cable sizes shown in Table 1 (95/180/240 mm²) is able to support three turbines, however only the cheapest option will be used in the algorithm solutions. Therefore, the two more expensive options are removed, keeping only the cheapest (180 mm²) as can be seen in Table 2. This process is repeated for cables supporting 1, 2, ..., up to N turbines with the resulting cable subset shown in Table 2. This reduced set of cables is made available to the algorithms and allows for the selection of cable rating based solely on the number of turbines being supported. Maintaining costs in a per-unit-length format ensures the selected cable sizes are of the lowest cost, regardless of connection length. This approach has been used in the academic literature, becoming a relatively standard method of considering electrical losses [9].

In order to further simplify the optimisation design, the number of possible connections - or arcs - are limited. Figure 1 shows an example containing 12 turbines and 1 substation, with Figure 1a containing all possible arcs and Figure 1b containing only the arcs from every turbine to its closest four turbines and the substation. As each arc represents a variable to be optimised by the optimisation algorithm, this method can greatly reduce the problem complexity, and for regular grid-based turbine layouts removing the longest arcs is highly unlikely to affect the optimal solution. Ensuring each turbine has an arc connecting it to a substation (regardless of the arc length) reduces the probability of infeasible solutions being generated and the risk of the

optimal solution being affected or removed. Of course, the constraints and intermediate solutions that are generated depend on the algorithm being used.

Before the longest arcs are removed, each arc route is checked to determine if it crosses the boundary of the wind farm, or an obstacle. If the arc does cross either of these, the length of that arc is artificially increased by a factor of 10 to penalise the route. These arcs are then highly likely to be removed during the reduction of the arc variables described previously.

2.2 | Mixed-integer linear programming (MILP)

The MILP method used in this study is based upon the methods proposed in [1] and [10]. In this method, binary variables are used to indicate whether a specific cable on a specific arc is present ($=1$) in the layout solution or not ($=0$), and other non-binary variables are included describing the power flow and branching costs. The optimisation problem was solved using Matlab R2018b and the built-in *intlinprog* function. The key processes used by the solver include: reducing the problem size with linear programming (LP) pre-processing; solving an initial relaxed (non-integer) problem with LP; tightening the LP relaxation with mixed-integer pre-processing; cut generation; heuristic methods to find an integer-feasible solution; and a branch-and-bound algorithm to solve the restricted formulation of the LP relaxation. The following sections outline the mathematical formulation of the objective function and the constraint equations.

2.2.1 | Objective function

The objective function aims to minimise the total lifetime cost of the installed network between all nodes, (i,j) , in the set of possible connections or arcs, \mathcal{A} , with the set of available cables, T . Denoting the cost as F , the optimisation problem is written as:

$$\min F = \sum_{(i,j) \in \mathcal{A}} \sum_{t \in T} c_{i,j}^t x_{i,j}^t \quad (2)$$

where $c_{i,j}^t$ is the cost of using a cable type t in the arc connecting nodes i and j (where cable type refers a specific combination of cable cross-sectional area and electrical loading scenario), and $x_{i,j}^t$ is a binary variable describing if cable type t is used for the arc connection (i,j) .

2.2.2 | Constraints

Kirchhoff's current law

A constraint must be applied in line with Kirchhoff's current law, stating that the current flowing into a node must

equal the current leaving the node, for all nodes in the set of nodes, V . This is implemented as seen in Equation (3), which states the power entering a node, P_{In} , plus the power generated at the node, P_{Gen} , must equal the power leaving the node, P_{Out} .

$$\sum_{i \in V} P_i = P_{In} + P_{Gen} - P_{Out} = 0 \quad (3)$$

No reverse power flow

In order to facilitate the Kirchhoff's current law constraint, Equation (3), the power flow in each arc must be calculated. An additional decision variable, $f_{i,j}$, describes the power flow in the arc (i,j) for all arcs in the set of arcs, \mathcal{A} , whose value is determined for each intermediate solution by the *intlinprog* solver concurrently with the remaining decision variables. Equation (4) applies a constraint to ensure that the power flow in a given cable section is greater than or equal to zero (implying directionality of connections). While, in reality, power may flow in either direction along a cable, the formulation presented in this study treats cables as having a 'direction'. This means that a cable connecting turbine A to turbine B will be considered separately to a cable connecting turbine B to turbine A, even though practically they are the same cable.

$$f_{i,j} \geq 0 \quad (4)$$

Cable rating

In order to prevent the overloading of cables, the rated capacity of a cable of type t , k_t , multiplied by the binary variable $x_{i,j}^t$ must be greater than or equal to the power flow in the arc, $f_{i,j}$, for all cable types in the set of cable types, T .

$$\sum_{t \in T} k_t x_{i,j}^t \geq f_{i,j} \quad (5)$$

Up to one cable can be used per arc

Equation (6) introduces a new binary decision variable, y , that describes if an arc is used by any cable type ($y = 1$) or remains unused ($y = 0$). By stipulating that y is equal to the sum of x variables associated with the same arc, this constraint restricts the maximum number of cables that can be used to one per arc.

$$\sum_{t \in T} x_{i,j}^t = y_{i,j} \quad (6)$$

No cables can leave and re-enter the same node

For simplicity, any arcs that leave and re-enter the same node are removed in pre-processing to avoid this possibility and to reduce the number of constraint equations.

Exactly one cable must leave a turbine

As the power leaving a turbine node cannot be split, and to ensure the power from a turbine is connected to a substation, Equation (7) stipulates that exactly one arc leaving a turbine

must be used, for all turbines in the set of turbine nodes, V_T .

$$\sum_{j \in V_T: i \neq j} y_{i,j} = 1, i \in V_T \quad (7)$$

No cables may leave a substation

As this optimisation is not considering export cable routing, a constraint may be applied to avoid any cables leaving a substation node, in a similar form to Equation (7). However, to reduce the number of constraint equations, any arcs leaving a substation node are removed during pre-processing.

Up to one cable may leave/enter a Steiner node

For any ‘empty’ (Steiner) nodes that are used to navigate around obstacles, it is important that only up to one cable is allowed to enter and leave the node. This is to avoid branched connections being employed at an effectively empty location rather than at a turbine node - resulting in unrealistic layouts. Equations (8) and (9) limit the number of connections entering and leaving Steiner nodes respectively, to less than or equal to one. In conjunction with Equation (3), if a cable enters a Steiner node, exactly one cable must leave the node. This is applied to all Steiner nodes in the set of Steiner nodes, V_0 .

$$\sum_{i \in V_0: i \neq j} y_{i,j} \leq 1, j \in V_0 \quad (8)$$

$$\sum_{k \in V_0: j \neq k} y_{j,k} \leq 1, j \in V_0 \quad (9)$$

Limit to the number of connections into turbines/substation(s)

Equations (10) and (11) limit the number of connections into substations and turbines to C and H respectively, where C and H are user-defined constants describing the maximum number of allowable connections. These constraints are useful to restrict solutions to use a realistic number of connections into a turbine, or avoid branched layouts altogether. Equations (10) and (11) are applied to all nodes in the set of substation nodes, V_{SS} , and all nodes in the set of turbine nodes, V_T , respectively.

$$\sum_{i \in V_0: i \neq j} y_{i,j} \leq C, j \in V_{SS} \quad (10)$$

$$\sum_{i \in V_0: i \neq j} y_{i,j} \leq H, j \in V_T \quad (11)$$

Cost of branched connections

As the connection of multiple strings into a single turbine requires more complex switch-gear and jointing, it is useful to be able to capture these costs in the optimisation process. Equation (12) introduces a binary variable, w_j^b , that describes whether b connections are connected into turbine j , ($w_j^b = 1$ if this condition is true). By including a cost coefficient, γ_b , for b connections this branching cost can be accounted for in the optimisation.

$$w_j^b \in \{0, 1\} \quad (12)$$

2.2.3 | Updating the objective function

In the previous section, several parameters were included for use in constraint equations, including: y_{ij} to describe if any cable is used in a given arc or connection, f_{ij} to describe the power flow in a given arc, w_j^b to describe if b connections enter turbine j , and γ_b to account for the cost of b connections into a turbine. As such, the objective function must be updated to include these terms. While the terms y and f are used in the constraint equations, they have no impact on the objective value and so can be given coefficients of zero. The cost of branched connections must be included, as shown in Equation (13), by summing the cost of b connections in the range of H (the limit of the number of connections) across all turbines in the set of turbines V_T . The updated objective function is written as:

$$\min \bar{F} = \left[\sum_{(i,j) \in A} \sum_{i \in T} c_{i,j}^t x_{i,j}^t + \sum_{b \in H} \gamma_b \sum_{j \in V_T} w_j^b \right] \quad (13)$$

2.3 | Classical ACO

The ant colony optimisation (ACO) algorithm mimics a colony of ants as they walk between their nest and a food source. Many different paths are taken by the ants as they search for food, depositing pheromones as they walk which can be detected by other ants. For destinations close to the nest, it will take less time for the ants to walk between the two sites and so the pheromone deposits are added more regularly, leading to a stronger concentration of the pheromone on that path. For an ant about to leave the nest, the probability that it will take a given path is proportional to the strength of the pheromone scent. Since the pheromones evaporate over time, the longer paths (on which pheromones are deposited less frequently) will be a less favourable option for other ants to take, resulting in a convergence to the most efficient path.

The ACO algorithm can be used to solve optimisation problems that can be formulated as a topological graph, which makes it well-suited to an array cable layout optimisation problem. In this study an ‘ant’ starts from the (unconnected) turbine that is furthest from a substation and undertakes a pseudo ‘random walk’ until it reaches a substation node. Another ant then starts at the unconnected turbine next-furthest from a substation, and undertakes a walk until it reaches a substation node or a turbine on an existing string. This is repeated until there are no turbines left unconnected. The available paths for the ants to take are constrained to reduce the number of decision variables in the optimisation. At each node, ants are able to walk (in a straight line) to the nearest 8 nodes, or directly to any substation node. The paths directly linked to substations are included to avoid an ant having no available path left to walk on - which may otherwise happen if all neighbouring turbines have been connected using a cable that has no remaining capacity to support an additional turbine.

An example iteration of the ACO algorithm is shown in Figure 2. Here the starting point (blue circle) can be considered

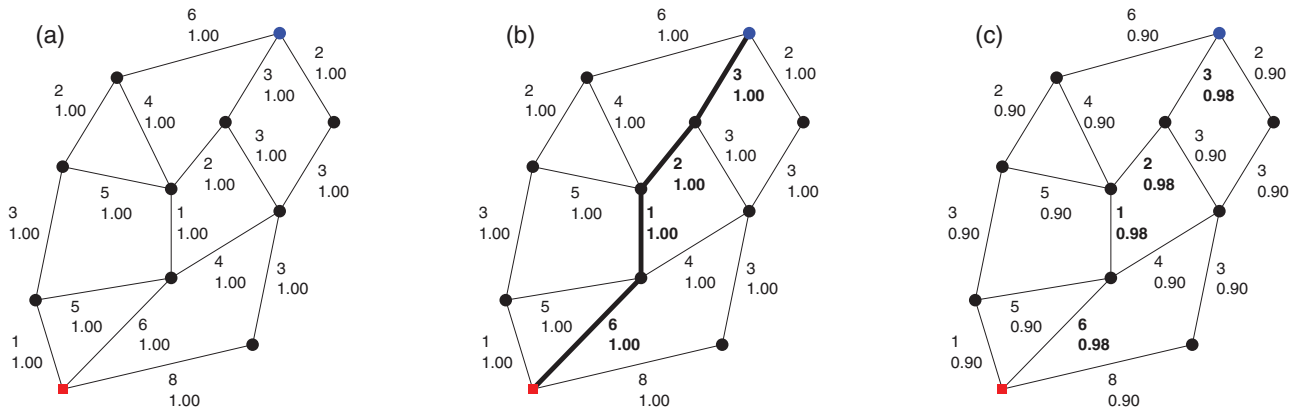


FIGURE 2 Example of a path taken by an ‘ant’ during an iteration of the ACO algorithm, from the start point (blue circle), via nodes (black circles), to the end point (red square). Path lengths and pheromone concentration are labelled for each path as the top and bottom numbers respectively, with (a) the initial conditions, (b) the path taken in bold, and (c) the updated pheromone concentrations

a turbine node, the end point (red square) can be considered as a substation node, and the remaining connecting nodes (black circles) can be considered ‘empty’/Steiner nodes. Figure 2a shows the initial conditions of the topological graph, with path lengths (or costs) and pheromone concentrations labelled for each path as the top and bottom number respectively. For an ant standing on node i , the probability of it walking to a connecting node j , via the path (or arc) $x_{i,j}$ is given by:

$$P_{x_{i,j}} = \frac{pher_{x_{i,j}} + weight_{x_{i,j}}}{\sum_{j \in J} (pher_{x_{i,j}} + weight_{x_{i,j}})} \quad (14)$$

where $pher_{x_{i,j}}$ is the pheromone concentration of the path x between nodes i and j , $weight_{x_{i,j}}$ is equal to the reciprocal of the cost of path $x_{i,j}$, and J is the set of nodes available to walk to from node i . Figure 2b shows an example of a completed path from the start node to the end node, with the paths that were selected shown in bold. Once a completed graph (connecting all turbines to a substation) has been generated, the pheromone concentrations must be updated. The pheromones on all paths are evaporated proportionally (10% evaporation ($evap = 0.9$) is used in the example in Figure 2).

$$pher_{x_{i,j}} = evap \times pher_{x_{i,j}} \quad (15)$$

where $evap$ is the evaporation constant. The objective value is then calculated and used to determine the pheromone deposit. In the example in Figure 2b the objective value (total cost of the route in this example) is equal to 12^* ($3+2+1+6$). The pheromone deposited on the used routes, $\Delta pher$, is equal to the reciprocal of the objective value, approximately 0.08.

$$\Delta pher = \frac{1}{F(x)} \quad (16)$$

Figure 2c shows the updated pheromone concentrations after the evaporation and deposit processes have taken place and the route has been cleared to begin the next iteration.

To adapt the algorithm to the optimisation problem under consideration and to improve the convergence behaviour, two adaptive parameters can be introduced into Equation (14) yielding Equation (17):

$$P_{x_{i,j}} = \frac{pher_{x_{i,j}}^\alpha + weight_{x_{i,j}}^\beta}{\sum_{j \in J} (pher_{x_{i,j}}^\alpha + weight_{x_{i,j}}^\beta)} \quad (17)$$

where α and β are exponents describing the pheromone constant and exploratory constant respectively. These two parameters weight the relative importance of the cost and pheromone strength of the paths and can be adjusted in the algorithm to reduce the time to convergence or increase the probability of new routes being explored. The overall ACO algorithm is summarised in Algorithm 1, where T_u is the set of unconnected turbines; $dist_{t_u, SS}$ is the distance between an unconnected turbine, t_u , and the closest substation, SS ; loc_{ant} is the location of the ant; N_v is the set of nodes that have been visited by an ant in the current iteration; ij are two nodes connected by a path (or arc) $x_{i,j}$ in the set of usable arcs \mathcal{A} ; \mathcal{A}_{used} is the subset of arcs that were used in a given iteration; $\bar{F}(x)$ is the updated objective function (Equation 13); and $avg\bar{F}$ is the average of the objective function which is averaged over m iterations and used to define the stopping criteria.

The values of the key parameters used in the ACO algorithm were initialised as: 1.00 for the pheromone concentration on all paths, $pher_{x_{i,j}}$; 0.50 for the pheromone exponent, α ; and 1.50 for the exploratory exponent, β . An evaporation constant of 0.99 was used.

2.4 | ACO with decomposition into sub-problems

Since the ACO algorithm creates an entirely new cable layout solution on each iteration, it is possible that improvements in one string, or area of the wind farm, go unnoticed due to a poor-quality section of the solution in other strings. This becomes

ALGORITHM 1 Ant colony optimisation algorithm

Initialise stopping criteria, $STOP = 0$, $n = 0$, $m = \text{length}(\text{nodes})$

while $STOP == 0$ **do**

$n = n + 1$

while $\text{length}(T_n) > 0$ **do**

Initialise ant at t_n with $\text{dist}_{t_n, SS} = \max(\text{dist}_{t_n, SS})$

while $\text{not}(loc_{ant} \in N_n)$ **do**

Calculate $P_{x_i, j}$ for $j \in J$

Roulette wheel selection to determine destination node, $j \in J$

Update ant location, $loc_{ant} = j$

end while

end while

Evaporate pheromone, $pber_{x_i, j} = pber_{x_i, j} \times \text{evap}$ for $x_i, j \in A$

Evaluate $\bar{F}(x)$

Calculate pheromone deposit, $\Delta pber$

Deposit pheromone, $pber_{x_i, j} = pber_{x_i, j} + \Delta pber$ for $x_i, j \in A$

Clear all routes, $x_{i, j} = 0$ for $x_{i, j} \in A$

if $n > m$ **then**

$\text{avg } \bar{F}_n = \text{mean}(\bar{F}(x)_{n-m} : \bar{F}(x)_n)$

if $n > 100m$ **and** $\text{avg } \bar{F}_{n-10m} \leq 1.01 \times \text{avg } \bar{F}_{n-m}$ **then**

$STOP = 1$

end if

end if

Return best layout, $\min(\bar{F})$

end while

increasingly true for larger problems where each string represents a smaller contribution to the total cost and therefore less influence on the pheromone to be deposited. The pheromone deposit is calculated from the total cost of the solution (objective value) and deposited equally on all of the paths used in an iteration. Therefore, the incentive (pheromone deposit) to use sections that have improved will be increased by the same amount as for those that have been made worse. In this section, an improved ACO algorithm, ACOsp, is proposed that considers small sub-problems of the larger optimisation problem, in a similar approach to simple decomposition techniques. In doing so, the algorithm is better able to notice improvements and apply more specific incentives for those routes to be used again.

Figure 3 shows how sub-problems are considered in this method. A section of a cable layout solution is shown, with turbine nodes (blue circles) and a substation node (red square) marked. Figure 3a contains an incumbent solution generated by a previous iteration, where two strings have been selected for consideration as a sub-problem, highlighted by the green region. The cable layout for turbines contained in the sub-problem is solved using Algorithm 1. The layout as a whole is considered in the objective function, Equation (13), however cables outside of the sub-problem region are fixed, and therefore the decision variables are limited to only those connections within the

sub-problem region. Figure 3b shows the incumbent solution with the cables in the sub-problem removed and all the possible connections to be considered, shown by the dotted lines, where the probability of a given path being selected is described in Equation (17). Connections are also present between the unconnected turbines and the substation, but have been omitted from the figure for clarity. It is important to note that the subset of decision variables to be considered in the sub-problem contains routes from the turbines in the sub-problem to all of their available connections, including other turbines outwith the sub-problem. Therefore, connections to neighbouring strings are also allowed to ensure turbines do not get stuck in one sub-problem region and that coupling between sub-problems is properly captured. Randomly selecting strings to create different sub-problems also helps to facilitate this improved search process. Figure 3c shows the best result found by the algorithm after the sub-problem has been optimised. It can be seen that several turbines have been connected to neighbouring strings outside of the sub-problem region and that one branched string connects the remaining turbines.

A new iteration begins by selecting random strings to form a sub-problem. The first string is selected randomly, then the remaining string(s) have a probability of being selected inversely proportional to their distance to the first string. This reduces the number of less-useful iterations where two strings at opposite ends of the wind farm are considered together as a sub-problem. String positions are defined as the average coordinate position of the turbines supported in that string. The probability that a string, s_2 , will be selected, following the random selection of the first string, s_1 , is given by:

$$P_{s_2} = \frac{1/\text{dist}(s_1, s_2)}{\sum_{s \in S} (1/\text{dist}(s_1, s_2))} \quad (18)$$

The overall optimisation algorithm, ACOsp, is summarised in Algorithm 2, where S_{rand} is the set of randomly selected string numbers used to create the sub-problem; T_{rand} is the set of turbine numbers in the sub-problem; s is a string number in the set S_{rand} ; and S_u is the set of binary values for all strings describing if a string has been ‘unimproved’ ($S_u(s) = 1$) or improved/not-yet-considered ($S_u(s) = 0$) by a sub-problem.

It can be seen in Algorithm 2 that the algorithm begins with a classical ACO approach to generate an initial solution. This phase is followed by the recursive decomposition where, at first, pairs of strings are selected to create sub-problems to be optimised. Once all combinations of pairs of strings have been considered together, and no further improvements can be found, the algorithm selects groups of three strings to create sub-problems - increasing the size of the solution space being searched by the algorithm. When three strings are being selected, the probability of selection is as presented in Equation (18), with the distance to the first—randomly selected—string being used. When all combinations of three strings yields no further improvements, the algorithms stopping criteria are met and the best solution (minimum objective value) will be output.

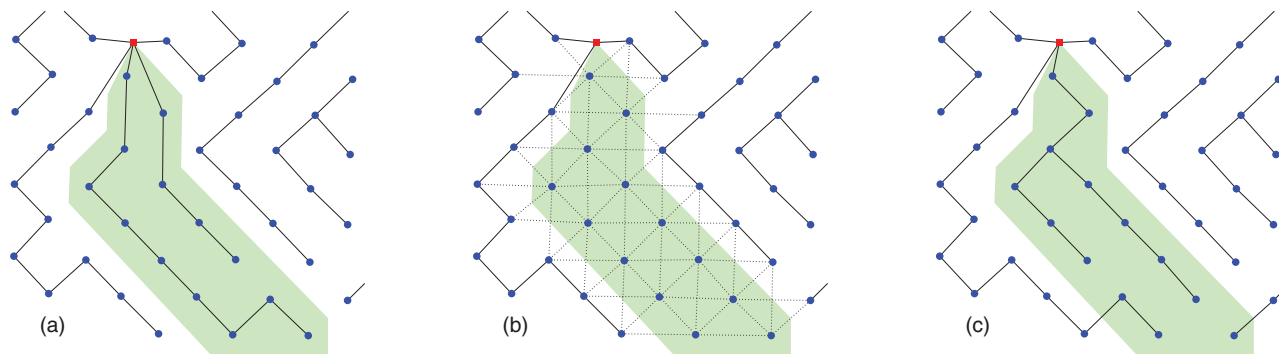


FIGURE 3 Example of a sub-problem in the improved ACOsp algorithm, with (a) two strings selected (green shaded area) to be considered as a sub-problem of the cable layout, (b) two original strings removed and the possible paths for the ACO algorithm shown by dotted lines (omitting connections to substation for clarity), and (c) the new solution comprising a single branched string and several turbines joining existing neighbouring strings

For the initial solution, and all further sub-problems, the ACO parameters were re-initialised. The initial pheromone concentration for all paths was 1.00, and the pheromone and exploratory exponents were set to 0.50 and 1.50 respectively. The evaporation constant was set to 0.99 for all phases of the algorithm.

3 | CASE STUDIES

This section details the case studies used for the comparison of the three optimisation algorithms described previously. Details of the large, hypothetical offshore wind farm site is provided and the six case studies based on the site are defined. Cost components used in the three optimisation approaches are presented including cable unit costs and additional key parameters necessary for the three algorithms.

3.1 | The hypothetical large offshore wind farm site

The offshore wind farm site under consideration is a large hypothetical site, proposed by the authors in a previous study investigating turbine layout optimisation [36] and contains full details of the wind farm boundary, obstacles and turbines. Figure 4 shows the hypothetical site, including the wind farm boundary, obstacles to be avoided by cables, and turbine and substation positions. The site contains 122 turbines to be connected through the array cable network to the two substations. Full details of the turbine coordinates can be found in the Appendix, Table A1.

The proposed site contains several aspects designed to be challenging for the cable layout optimisation algorithms. Firstly, the wind farm boundary is an irregular shape including concave edges for cables to navigate around, which incurs a penalty cost if crossed by cables. Secondly, obstacles are included in the site (Figure 4 red shaded regions), which also incurring a penalty cost if cables cross any obstacle boundary. Steiner nodes are included at some of the convex vertices of the obstacles to allow cables to navigate around them (Figure 4 green

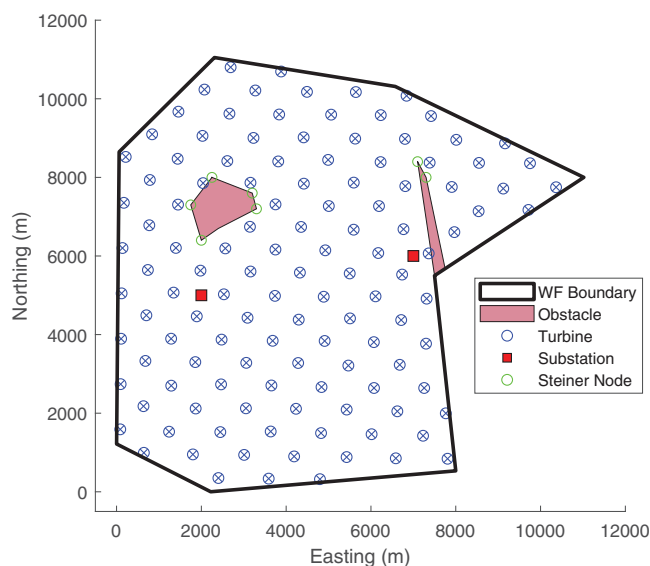


FIGURE 4 The hypothetical GW-scale offshore wind farm test case

circles). Thirdly, two substations are employed (Figure 4 red squares) due to the large number of turbines which adds complexity to the cable network solution. Finally, one substation is placed very close to the eastmost obstacle, resulting in a difficult connection to turbines on the opposite side of the obstacle. The Easting-Northing coordinates of the two substations are (2000 m, 5000 m) and (7000 m, 6000 m).

3.2 | Definition of the six case studies

Six test cases are created from the hypothetical site, containing 10, 15, 25, 40, 61, and 122 turbines respectively. Figure A1, in the Appendix, shows the turbine positions used for these 6 test cases. Including case studies on a range of numbers of turbines allows for the assessment of the algorithms' performance and how these scales with problem complexity. Although the cases with fewer turbines may appear simple, beginning with those in the north-east section requires the algorithm to con-

ALGORITHM 2 Ant colony optimisation algorithm with decomposition strategy

```

Initialise stopping criteria,  $STOP = 0$ 
while  $length(T_n) > 0$  do
  Initialise ant at  $t_u$  with  $dist_{t_u, ss} = \max(dist_{t_u, ss})$ 
  while  $not(loc_{ant} \in N_v)$  do
    Calculate  $P_{x_{i,j}}$  for  $j \in J$ 
    Roulette wheel selection to determine destination node,  $j \in J$ 
    Update ant location,  $loc_{ant} = j$ 
  end while
end while
for  $n = 2 : 3$  do
  while  $STOP2 = 0$  do
    Randomly select  $n$  strings,  $S_{rand}$ , (connecting turbines,  $T_{rand}$ )
    Clear cables in the selected strings,  $x_{i,j} = 0$  for  $i \in T_{rand}$ 
    Run Algorithm 1(considering all  $T$ , but clearing only  $x_{i,j}$  for  $i \in T_{rand}$ )
    Record best layout to date,  $\min(\bar{F})$ 
    for  $s \in S_{rand}$  do
      if String  $s$  is unimproved,  $cost(s) > \min(cost(s))$  then
         $S_u(s) = 1$ 
      end if
    end for
    if  $\sum S_u = length(S_u)$  then
       $STOP2 = 1$ 
    end if
  end while
   $S_u = 0$ 
   $STOP2 = 0$ 
end for
Return best layout,  $\min(\bar{F})$ 

```

TABLE 3 Key cable parameters

Cable number	Cable power capacity (MW)	Unit cost (£/m)	Resistance (Ω /m)
1	60	1400	0.030
2	90	1750	0.014
3	100	1870	0.011

sider the wind farm boundary, obstacles, and Steiner nodes for all problem cases. Both substations are kept for all cases.

3.3 | Cost components and parameters

Table 3 contains the key parameters of the three cables that are available for the optimisation algorithm to use. Cable power capacity is used to limit the number of turbines supported by a cable and is a restating of the current carrying capacity. The

TABLE 4 Key parameters and values used in the cable layout optimisation comparison

Parameter	Value
Array voltage	66 kV
Crossing penalty	£1 M
Jointing cost (turbines)	£13.8k
Jointing cost (substation)	£90.7k
Price of energy	£50/MWh
Discount rate	10%
Project lifetime	25 years
Nearest N nodes of allowable connections	8

capacity, unit cost, and resistance per unit length of each cable are representative values proposed by the authors and are not taken from specific real cables.

Table 4 contains further parameters for the optimisation algorithms to consider. Similarly to cable cost information in Table 3, the values described in Table 4 are mostly representative values selected by the authors used for this study. The crossing penalty represents an increase in cost due to cables crossing other cables and is discussed further in the following section. A jointing cost is included for connections into turbines and substations. While one connection to either of these incurs zero additional cost, every additional connection increases the network cost by £13.8k [10] and £90.7k [4], for connections to turbines and substations respectively. Although this cost function is linear, it would be trivial to include a more realistic non-linear cost function in future studies. The price of energy, discount rate, and project lifetime are used to calculate the electrical losses in the pre-computation phase described previously in Section 2.1. Additionally, in the pre-processing phase, the set of arcs is reduced by considering only connections between the nearest N neighbours. For this study the connections between the closest eight neighbours were kept in the set of possible connections. In addition, all connections directly to substations were also retained in the set of arcs.

4 | RESULTS AND DISCUSSION

This section presents the results of the three optimisation algorithms with comparison of the solutions and computational time. Consideration of crossing cables is presented for one of the cases with a crossing cable in the optimal solution before the penalty cost and/or constraint is applied.

4.1 | Comparison of the three algorithms

The three optimisation algorithms were run on a standard desktop computer (3.4 GHz Intel Core i7-6700, 16 GB RAM) and ten simulations were conducted for each algorithm on each of the six case studies. Table 5 contains the averaged results of each algorithm for each of the six case studies. Objective values are presented with the optimality ratio (which is a ratio between a

TABLE 5 Average results of the three optimisation methods for the six hypothetical test cases. (Results in italics indicate an unfinished result)

No. turbines	Objective value (£) and optimality ratio			Computational time (s)		
	MILP	ACO	ACOSP	MILP	ACO	ACOSP
10	22,064,833 (1.000)	22,667,188 (1.027)	22,068,446 (1.000)	3	5	53
15	30,945,049 (1.000)	31,075,301 (1.004)	30,945,049 (1.000)	9	8	46
25	50,235,935 (1.000)	51,473,967 (1.025)	50,750,255 (1.010)	31	18	133
40	68,683,109 (1.000)	69,693,934 (1.015)	69,678,545 (1.014)	204	51	489
61	103,255,681 (1.000)	110,766,917 (1.073)	104,651,892 (1.014)	951	164	1517
122	<i>197,401,005 (1.000)</i>	212,339,986 (1.076)	199,301,590 (1.010)	<i>13717</i>	833	9991

solution and the optimal solution) and the average computational time is shown for each case. The optimal solution for comparison is obtained through the MILP algorithm with the final 'branch and bound' section of the algorithm running until optimality is reached. This is not reached for the case of 122 turbines but the value is assumed to be optimal, discussed further later. A complete set of results can be found in the Appendix, Tables A2 and A3. It can be seen in Table 5 that the MILP algorithm finds the mathematically optimal solution for almost all cases. However, the computational time increases significantly as the number of turbines (and therefore number of possible cable connections) increases. For the largest case study, containing 122 turbines, the MILP algorithm is unable to prove the optimality of the solution due to the large memory requirements of the branch-and-bound solver. The total memory available to hold data on the standard desktop computer was 37,101 MB. This was sufficient to record all intermediate solutions for the case of 61 turbines, but not for the case of 122 turbines.

The results from the classical ACO algorithm are between 0.4% and 7.6% more expensive than the optimal solution as assessed by the objective function, averaging 3.7% greater cost than the optimal solutions across the 6 case studies. The proposed ACOSP solutions are between 0.0% and 1.4% more expensive than the optimal solutions and 0.8% greater cost than the optimal solutions on average across the 6 case studies. There is some indication that as the problem complexity increases, the average optimality ratios of the ACO and ACOSP solutions increase. This can be seen most significantly in the classical ACO solutions, suggesting that the proposed ACOSP method is better at handling larger problems than the classical ACO method.

The computational time for the ACO and ACOSP methods increases less quickly than the MILP algorithm, as the number of turbines increases. For all six cases, except for the smallest (ten turbines), the classical ACO method is the quickest to converge to a solution. However, since all the computational times are reasonably low (of the order of a few hours), the ACOSP algorithm is considered to be an appropriate method for solving large scale problems using standard desktop computing. Clearly for smaller problems, the MILP algorithm performs the best - yielding optimal solutions in reasonable computational time.

Figure 5 shows the cable routing solutions of the three methods, for the case containing all 122 turbines. Some similarities

can be seen between the three layouts, however they are largely different. This is due to the regular spacing of the turbines resulting in very different layouts with near-optimal total cost, and algorithms reaching a local-minimum which they fail to improve before the stopping criteria are met. Information on the cable types used in the layout are omitted from Figure 5 for clarity. All three algorithms shared a common pre-optimisation computing phase and cable selection process. As such, cable ratings for sections supporting the same number of turbines are the same across solutions.

Table 5 shows that the major limitation of the MILP method is the large increase in computational time and memory with increasing number of turbines. Both ACO approaches offer a quicker alternative to this MILP approach. However, the average optimality of all ACO solutions is 1.037, meaning solutions are 3.7% more expensive than the optimal solutions on average. This compromise for quicker computational time is still present in the ACOSP algorithm, however it has an average optimality across all solutions of 1.008, which translates to an increase in cost of 0.8% relative to the optimal solutions. Therefore, the simulation results show the proposed ACOSP algorithm is an effective tool for solving large cable layout optimisation problems in a reasonable time period.

Initially, only the arcs crossing the wind farm boundary and/or an obstacle are penalised as described previously in the pre-processing phase. Cables crossing other cables are handled differently as they may or may not be present in a given solution. Figure 6 shows the optimal cable routing for the case of 25 turbines when cable crossings are not considered, with Figure 6a showing the whole solution and Figure 6b showing a zoomed-in section to identify the crossing connections. In order to avoid such crossing sections, constraints must be applied to the solution space containing the set of all possible solutions.

4.2 | Considering crossing cables

Since there are many possible arcs that can be used in the cable routing solution, there are a large number of possible crossing arc pairs to be avoided (of the order \mathcal{A}^2). This means that applying constraints for each combination in the pre-processing phase is impractical. As such, constraints are applied on-the-fly and are considered differently for the MILP algorithm and the ACO-based algorithms.

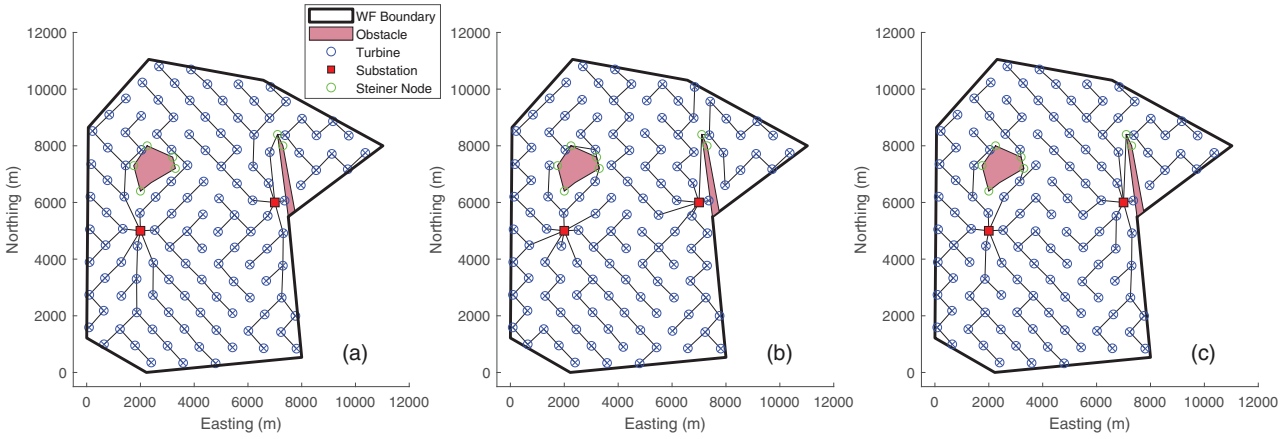


FIGURE 5 Optimised cable layouts from (a) the MILP algorithm, (b) the classical ACO algorithm, and (c) the ACO algorithm with sub-problems. All MILP layouts were identical, solutions for (b) and (c) use the first layout out of the set of layouts generated

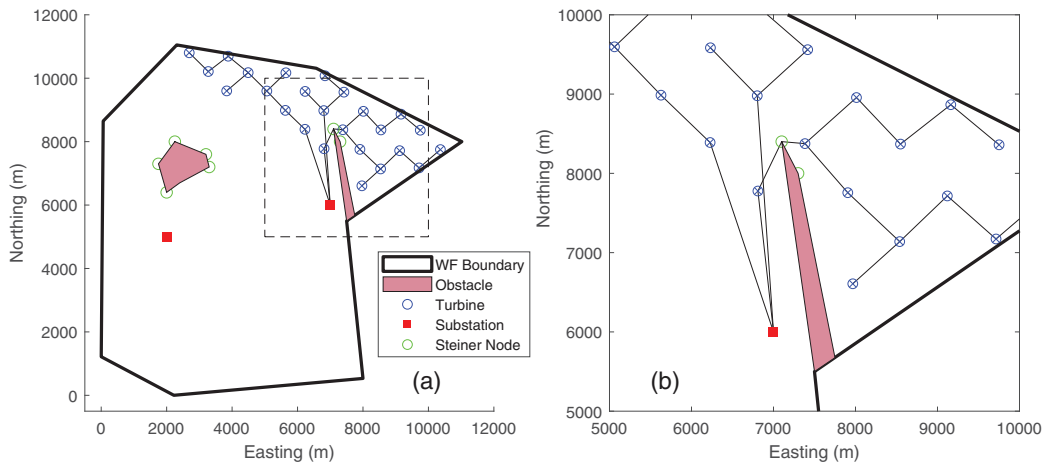


FIGURE 6 Optimal cable layout for 25 turbines (a) full cable layout, and (b) a zoomed section of the layout to show the crossing cables

For the MILP algorithm, a solution is generated as described in Section 2.2. The solution is then checked for crossing cables by solving simultaneous equations of the two straight-line connections to determine if the intercept lies within the region covered by the two cables. This is only conducted for the cables that are used in the solution and not for all possible arcs. If a pair of crossing cables is present in the solution, a constraint equation is created limiting the solution to contain up to one of the pair of cables. An additional constraint equation is included for every pair of crossing cables present in the solution. Equation (19) describes the constraint equation used in the MILP algorithm.

$$y_{i,j} + y_{j,i} + y_{k,l} + y_{l,k} \leq 1, \{i, j\}, \{k, l\} \in B \quad (19)$$

where $y_{i,j}$ and $y_{j,i}$ are the two arcs between nodes i and j , $y_{k,l}$ and $y_{l,k}$ are the two arcs between nodes k and l , and B is the set of crossing arc pairs. The sum of the number of connections used for a given pair of crossing arcs, considered in both directions, must be less than or equal to one, for all arc pairs within the set of crossing arc pairs. Once all required constraint equations are

included, the MILP algorithm is re-run to generate a solution that obeys the new constraint equations.

The two ACO-based algorithms also describe a set of crossing arcs, B , which is initialised as an all-zero matrix. There is a complementary matrix of the same size, B_{idx} , that describes whether pairs of arcs have been assessed to determine if they cross, all values of which are also initialised to be zero. For every iteration of both algorithms, the quality of the solution is assessed as outlined in Section 2. During this assessment, all arcs are checked for crossing cables and marked in the index matrix, B_{idx} , to record that they have been checked (cell value = 1). If the pair of cables that are being checked do cross, then the penalty cost is recorded in the corresponding cell in the matrix of crossing edges, B , and the penalty cost is added to the cost of the solution. Since the objective of this penalty cost is to avoid crossing cable connections, it is given an arbitrary but relatively high value of £1 M, Table 4. This is repeated for all cable pairs in the current solution. For future iterations, if a cable pair have previously been checked, any penalty cost can be found in the matrix B . This avoids repeating the calculations required to check if pairs of cables cross, avoiding unnecessary

TABLE 6 Average results of the 3 optimisation methods for the hypothetical test case of 25 turbines, (a) without the cable crossing constraint, (b) with the cable crossing constraint. The values in () are the optimality ratios

No. turbines	Objective value (£) (Optimality ratio)			Comp. time (s)		
	MILP	ACO	ACOSP	MILP	ACO	ACOSP
25 (a)	50,235,935 (1.000)	51,473,967 (1.025)	50,750,255 (1.010)	31	18	133
25 (b)	50,268,994 (1.000)	51,307,620 (1.021)	50,826,954 (1.011)	78	31	243

computational expense. The objective values and computational time of the solutions from the three algorithms—with and without the cable crossing constraint/penalty—is shown in Table 6. A complete set of results is provided in the Appendix, Table A4.

Including the crossing cables constraint increased the computational time of the MILP algorithm by approximately a factor of 2. This shows that, upon including the constraint to avoid the crossing pair of cables, the optimal solution in the newly constrained case did not contain any further crossing cables. The optimal solution of the constrained case increased costs by £33,059 compared to beforehand with no cable crossing constraint. Both ACO-based algorithms demonstrated an increase in computational time, with the crossing constraint cases taking just under twice as long as previously. The optimality ratios of both ACO-based methods also remain relatively unchanged, providing confidence in the handling of the crossing cables and the effectiveness of the penalty function. The ACOSP algorithm remained the lowest cost solution of the two ACO-based approaches, being 1.1% higher cost than the optimal cable routing.

5 | CONCLUSIONS

In this work, a new heuristic optimisation algorithm, ACOSP, is proposed based on combined techniques in ACO and decomposition of a large network, to tackle the large-scale cable layout optimisation design problem for offshore wind farms. This proposed algorithm is compared with the MILP algorithm and a standard ACO algorithm. Through the comparison of the three algorithms, the MILP method was shown to reach the optimal solution in most case study scenarios. However, as the number of turbines and possible arc connections increases, the computational time and memory requirements of the MILP algorithm increase dramatically until it is no longer a practical approach. The classical ACO algorithm has shown to be a useful alternative, not suffering from the same memory and time constraints as the MILP algorithm. The ACO algorithm generated solutions between 0.4% and 7.6% more expensive than the optimal solution and was the quickest of the three algorithms in all cases except for the smallest one (10 turbines). The proposed ACOSP algorithm demonstrated increased performance in the quality of solutions, with solutions between 0.0% and 1.4% more expensive than the MILP optimal solution. While the improved solutions from the ACOSP algorithm did take a longer time to run, the algorithm completed all case studies within a few hours and so the computational time appears to be a reasonable

trade-off for the marked increase in the quality of the solutions. In this regard, the ACOSP algorithm should be a good alternative for very large wind farms when only standard computing facilities are available.

This study contained several assumptions and simplifications that may be of interest to future studies in this area of research. Firstly, arcs were limited to straight-line connections, which for offshore wind farms is a reasonable simplification. However, including a path-finding algorithm to define arc routes before the optimisation would allow for more detailed bathymetry and obstacles to be included. This may also help to avoid crossing cables as was seen in the original solution of the case with 25 turbines. Secondly, crossing cables were not accepted in the solutions through the use of constraints or penalty functions. Applying a penalty function that is indicative of the actual costs associated with crossing cables would allow the algorithms to determine if the increase in costs due to added protection at the crossing is offset by the reduction in length and capital cost. Thirdly, all turbines were assumed to generate the same electrical power regardless of their position in the array. Including a simple aerodynamic wind farm model would allow a more accurate representation of the power carried by the cables and therefore more accurate electrical losses to be determined. Finally, the impact of different sub-problem construction and the effect on the optimality of solutions would be a valuable future study. In this study, the decomposition was informed by the problem formulation (i.e. selecting a subset of decision variables by selecting strings of turbines to form a sub-problem). However, other methods of selecting decision variables could affect solutions, such as random selection of a given percentage of decision variables.

CONFLICT OF INTEREST

There is no conflict of interest.

DATA AVAILABILITY STATEMENT

The data that support the findings of this study are available from the corresponding author upon reasonable request.

ORCID

Peter Taylor  <https://orcid.org/0000-0002-2433-6719>

REFERENCES

1. Fischetti, M., Pisinger, D.: Optimizing wind farm cable routing considering power losses. *Eur. J. Oper. Res.* 270(3), 917–930 (2018). <https://doi.org/10.1016/j.ejor.2017.07.061>

2. Serrano González, J., Burgos Payán, M., Santos, J.M.R., González-Longatt, F.: A review and recent developments in the optimal wind-turbine micro-siting problem. *Renewable Sustainable Energy Rev.* 30, 133–144 (2014). <https://linkinghub.elsevier.com/retrieve/pii/S1364032113006989>
3. Quinonez-Varela, G., Ault, G., Anaya-Lara, O., McDonald, J.: Electrical collector system options for large offshore wind farms. *IET Renewable Power Gener.* 1(2), 107 (2007). https://digital-library.theiet.org/content/journals/10.1049/iet-rpg_20060017
4. Dicorato, M., Forte, G., Pisani, M., Trovato, M.: Guidelines for assessment of investment cost for offshore wind generation. *Renewable Energy.* 36(8), 2043–2051 (2011). <http://doi.org/10.1016/j.renene.2011.01.003>
5. Eriksson, E., Wind farm layout—A reliability and investment analysis, Ph.D. dissertation, Uppsala University (2008)
6. Catmull, S., Chippendale, R.D., Pilgrim, J.A., Hutton, G., Cangy, P.: Cyclic load profiles for offshore wind farm cable rating. *IEEE Trans. Power Delivery* 31(3), 1242–1250 (2016). <http://ieeexplore.ieee.org/document/7208884/>
7. Đorđević, A., Đurišić, Ž.: General mathematical model for the calculation of economic cross sections of cables for wind farms collector systems. *IET Renewable Power Gener.* 12(8), 901–909 (2018). <https://onlinelibrary.wiley.com/doi/10.1049/iet-rpg.2017.0420>
8. Pereira, T., Castro, R.: Comparison of internal grid topologies of offshore wind farms regarding reliability and economic performance metrics analysis. *IET Renewable Power Gener.* 13(5), 750–761 (2019)
9. Fischetti, M., Pisinger, D.: On the impact of using mixed integer programming techniques on real-world offshore wind parks. In: *Proceedings of the 6th International Conference on Operations Research and Enterprise Systems (ICORES 2017)*(Icores), Porto, Portugal, pp. 108–118 (2017)
10. Fischetti, M., Pisinger, D.: Optimal wind farm cable routing: Modeling branches and offshore transformer modules. *Networks* 72(1), 42–59 (2018). <https://onlinelibrary.wiley.com/doi/10.1002/net.21804>
11. Pérez-Rúa, J.A., Lumberras, S., Ramos, A., Cutululis, N.A.: Reliability-based topology optimization for offshore wind farm collection system. *Wind Energy.* 25(1), 52–70 (2021)
12. Fischetti, M., Pisinger, D.: Mixed integer linear Programming for new trends in wind farm cable routing. *Electron. Notes Discrete Math.* 64, 115–124 (2018). <https://doi.org/10.1016/j.endm.2018.01.013>
13. Pillai, A.C., Chick, J., Johanning, L., Khorasanchi, M., De Laleu, V.: Offshore wind farm electrical cable layout optimization. *Eng. Optim.* 47(12), 1689–1708 (2015). <https://doi.org/10.1080/0305215X.2014.992892>
14. Pillai, A., Chick, J., Johanning, L., Khorasanchi, M., Pelissier, S.: Optimisation of offshore wind farms using a genetic algorithm. *Int. J. Offshore Polar Eng.* 26(3), 225–234 (2016). <http://legacy.isope.org/publications/journals/journalSeptember16.htm>
15. Fischetti, M., Pisinger, D.: Mathematical optimization and algorithms for offshore wind farm design: An overview. *Bus. Inf. Syst. Eng.* 61, 469–485 (2018)
16. Hertz, A., Marcotte, O., Mdimagh, A., Carreau, M., Welt, F.: Optimizing the design of a wind farm collection network. *INFOR: Inf. Syst. Oper. Res.* 50(2), 95–104 (2012). <https://www.tandfonline.com/doi/full/10.3138/infor.50.2.095>
17. Cerveira, A., Pires, E.J., Baptista, J.: Wind farm cable connection layout optimization with several substations. *Energies* 14(12), 1–14, (2021)
18. Bauer, J., Lysgaard, J.: The offshore wind farm array cable layout problem: A planar open vehicle routing problem. *J. Oper. Res. Soc.* 66(3), 360–368 (2015)
19. Qi, Y., Hou, P., Liu, G., Jin, R., Yang, Z., Yang, G., Dong, Z.: Cable connection optimization for heterogeneous offshore wind farms via a voronoi diagram based adaptive particle swarm optimization with local search. *Energies* 14(3), 644 (2021)
20. Dutta, S., Overbye, T.J.: A clustering based wind farm collector system cable layout design. In: *2011 IEEE Power and Energy Conference at Illinois, PECEI 2011*, Urbana, IL, pp. 4–9 (2011)
21. Shin, J.-S., Kim, J.-O.: Optimal design for offshore wind farm considering inner grid layout and offshore substation location. *IEEE Trans. Power Syst.* 32(3), 2041–2048 (2017). <http://ieeexplore.ieee.org/document/7519100/>
22. Wu, Y., Zhang, S., Wang, R., Wang, Y., Feng, X.: A design methodology for wind farm layout considering cable routing and economic benefit based on genetic algorithm and GeoSteiner. *Renewable Energy.* 146, 687–698 (2020). <https://doi.org/10.1016/j.renene.2019.07.002>
23. Cazzaro, D., Pisinger, D.: Balanced cable routing for offshore wind farms with obstacles. *Networks* (2022)
24. Gonzalez-Longatt, F.M., Wall, P., Regulski, P., Terzija, V.: Optimal electric network design for a large offshore wind farm based on a modified genetic algorithm approach. *IEEE Syst. J.* 6(1), 164–172 (2012). <http://ieeexplore.ieee.org/document/6007042/>
25. Zuo, T., Zhang, Y., Meng, K., Tong, Z., Dong, Z.Y., Fu, Y.: A Two-layer hybrid optimization approach for large-scale offshore wind farm collector system planning. *IEEE Trans. Ind. Inf.* 17(11), 7433–7444 (2021)
26. Wędzik, A., Siewierski, T., Szypowski, M.: A new method for simultaneous optimizing of wind farm's network layout and cable cross-sections by MILP optimization. *Appl. Energy* 182, 525–538 (2016). <http://doi.org/10.1016/j.apenergy.2016.08.094>
27. Cerveira, A., de Sousa, A.F., Pires, E.J., Baptista, J.: Optimal cable design of wind farms: The infrastructure and losses cost minimization case. *IEEE Trans. Power Syst.* 31(6), 4319–4329 (2016)
28. Fischetti, M., Pisinger, D.: On the impact of considering power losses in offshore wind farm cable routing. In: *Communications in Computer and Information Science.* Vol. 50 Springer International Publishing, Berlin, pp. 267–292 (2018)
29. Dorigo, M., Di Caro, G.: Ant colony optimization: A new meta-heuristic. In: *Proceedings of the 1999 Congress on Evolutionary Computation-CEC99 (Cat. No. 99TH8406)*, Washington, DC, pp. 1470–1477 (1999). <http://ieeexplore.ieee.org/document/782657/>
30. Wu, Y.-K., Lee, C.-Y., Chen, C.-R., Hsu, K.-W., Tseng, H.-T.: Optimization of the wind turbine layout and transmission system planning for a large-scale offshore WindFarm by AI technology. *IEEE Trans. Ind. Appl.* 50(3), 2071–2080 (2014). <http://ieeexplore.ieee.org/document/6607158/>
31. Srikakulapu, R., Vinatha, U.: Combined approach based on ACO with MTSP for optimal internal electrical system design of large offshore wind farm. In: *2018 International Conference on Power, Instrumentation, Control and Computing (PICC)*, Thrissur, India, pp. 1–6 (2018). <https://ieeexplore.ieee.org/document/8384743/>
32. Lumberras, S., Ramos, A.: Offshore wind farm electrical design: A review. *Wind Energy.* 16(3), 459–473 (2013). <http://doi.wiley.com/10.1002/we.1498>
33. Hendrix, E.M., G-Tóth, B.: Introduction to Nonlinear and Global Optimization, ser. Springer Optimization and Its Applications, Springer New York, New York, NY (2010). <http://link.springer.com/10.1007/978-0-387-88670-1>
34. Fischetti, M., Pisinger, D.: Inter-array cable routing optimization for big wind parks with obstacles. In: *2016 European Control Conference, ECC 2016*, Aalborg, Denmark, pp. 617–622 (2017)
35. Lumberras, S., Ramos, A.: Optimal design of the electrical layout of an offshore wind farm applying decomposition strategies. *IEEE Trans. Power Syst.* 28(2), 1434–1441 (2013)
36. Taylor, P., Yue, H., Campos-Gaona, D., Anaya-Lara, O., Jia, C.: Turbine layout optimisation for large-scale offshore wind farms—A grid-based method. *IET Renewable Power Gener.* 15(16), 3806–3822 (2021). <https://onlinelibrary.wiley.com/doi/10.1049/rpg2.12295>

How to cite this article: Taylor, P., Yue, H., Campos-Gaona, D., Anaya-Lara, O., Jia, C.: Wind farm array cable layout optimisation for complex offshore sites—A decomposition based heuristic approach. *IET Renew. Power Gener.* 17, 243–259 (2023). <https://doi.org/10.1049/rpg2.12593>

APPENDIX A

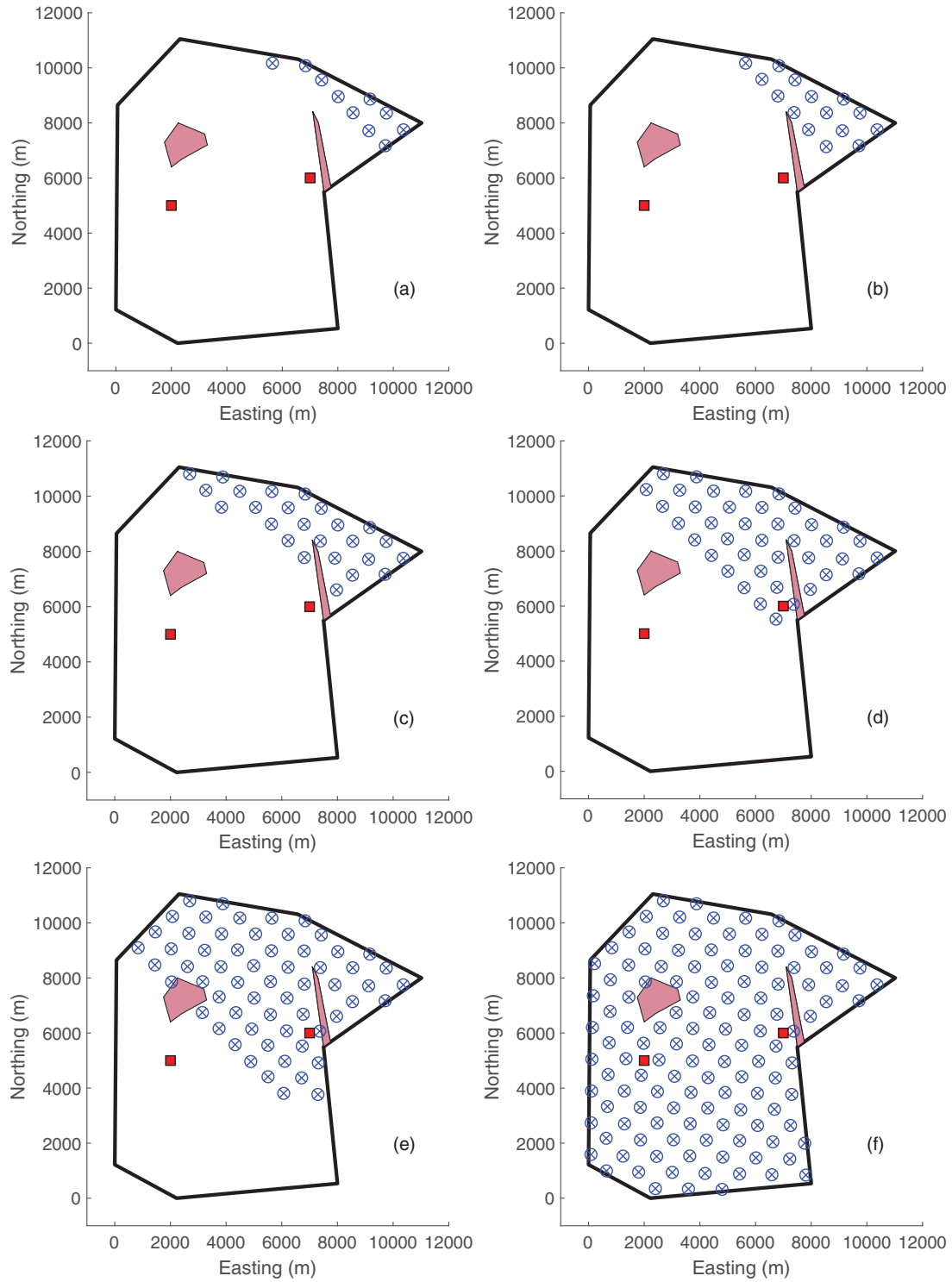


FIGURE A1 Test cases of the hypothetical offshore wind farm site, with (a) 10 turbines, (b) 15 turbines, (c) 25 turbines, (d) 40 turbines, (e) 61 turbines, (f) 122 turbines. Steiner nodes omitted for clarity

TABLE A1 Turbine positions for cable layout optimisation comparison

No.	x-coord. (m)	y-coord. (m)	No.	x-coord. (m)	y-coord. (m)	No.	x-coord. (m)	y-coord. (m)
1	9162	8866	42	1459	9672	83	3089	4428
2	9751	8360	43	2027	9056	84	3682	3842
3	10366	7749	44	2612	8415	85	4283	3277
4	6840	10077	45	3158	7863	86	4834	2665
5	7417	9560	46	3749	7313	87	5427	2092
6	8012	8956	47	4352	6739	88	6015	1465
7	8549	8369	48	4923	6144	89	6586	852
8	9120	7715	49	5499	5556	90	140	6202
9	9714	7172	50	6108	4973	91	739	5644
10	5644	10171	51	6713	4370	92	1345	5068
11	6231	9584	52	7299	3769	93	1892	4464
12	6802	8979	53	839	9096	94	2477	3872
13	7384	8375	54	1441	8473	95	3059	3281
14	7906	7756	55	2041	7854	96	3652	2705
15	8539	7139	56	3146	6743	97	4232	2112
16	3881	10694	57	3747	6164	98	4823	1494
17	4491	10176	58	4324	5577	99	5426	883
18	5061	9596	59	4886	4963	100	119	5049
19	5628	8986	60	5506	4412	101	703	4491
20	6227	8389	61	6068	3808	102	1287	3895
21	6810	7777	62	6679	3231	103	1857	3300
22	7967	6607	63	7255	2641	104	2465	2733
23	2690	10802	64	7765	1997	105	3051	2124
24	3273	10211	65	216	8521	106	3635	1534
25	3835	9600	66	785	7934	107	4188	900
26	4412	9018	67	1450	7307	108	4797	321
27	4990	8445	68	2565	6193	109	107	3894
28	5594	7867	69	3159	5605	110	680	3330
29	6190	7270	70	3736	4985	111	1290	2700
30	6767	6682	71	4296	4380	112	1866	2119
31	7362	6066	72	4908	3838	113	2447	1519
32	2073	10234	73	5467	3212	114	3009	939
33	2662	9622	74	6072	2641	115	3588	335
34	3229	9004	75	6622	2048	116	96	2739
35	3813	8406	76	7229	1426	117	635	2178
36	4417	7840	77	7807	841	118	1239	1529
37	5006	7271	78	172	7353	119	1800	951
38	5592	6669	79	772	6782	120	2402	350
39	6172	6075	80	1399	6205	121	87	1589
40	6735	5527	81	1979	5627	122	644	992
41	7313	4914	82	2531	5025			

TABLE A2 Full results of the 3 cable layout optimisation methods for the hypothetical test cases of 10, 15, 25, and 40 turbines

No. turbines	Objective value (£) (Optimality ratio)			Comp. time (s)		
	MILP	ACO	ACOsp	MILP	ACO	ACOsp
10	22,064,833	22,408,394	22,064,833	2	5	56
10	22,064,833	22,218,796	22,064,833	3	5	62
10	22,064,833	22,818,266	22,064,833	3	5	43
10	22,064,833	23,390,878	22,064,833	2	5	56
10	22,064,833	22,082,901	22,082,901	3	5	59
10	22,064,833	23,065,385	22,064,833	3	5	52
10	22,064,833	22,064,833	22,064,833	3	5	44
10	22,064,833	23,688,668	22,064,833	3	5	34
10	22,064,833	22,850,863	22,082,901	3	5	59
10	22,064,833	22,082,901	22,064,833	3	5	65
15	30,945,049	30,945,049	30,945,049	9	8	46
15	30,945,049	30,962,130	30,945,049	9	8	42
15	30,945,049	30,945,049	30,945,049	9	8	48
15	30,945,049	30,945,049	30,945,049	9	8	44
15	30,945,049	30,945,049	30,945,049	9	8	37
15	30,945,049	30,945,049	30,945,049	9	8	36
15	30,945,049	30,981,350	30,945,049	9	8	42
15	30,945,049	31,473,244	30,945,049	9	8	84
15	30,945,049	31,318,610	30,945,049	9	8	33
15	30,945,049	31,292,432	30,945,049	9	8	46
25	50,235,935	51,400,208	50,726,894	32	18	184
25	50,235,935	51,082,109	50,517,433	31	18	184
25	50,235,935	51,435,071	50,906,992	32	19	117
25	50,235,935	50,726,894	50,638,853	30	19	130
25	50,235,935	50,986,235	51,120,941	31	19	84
25	50,235,935	52,211,013	50,863,738	31	19	153
25	50,235,935	52,834,868	50,638,853	31	19	152
25	50,235,935	51,298,347	51,002,778	31	18	114
25	50,235,935	50,986,235	50,254,400	31	19	96
25	50,235,935	51,778,689	50,831,666	31	18	118
40	68,683,109	69,616,813	68,773,414	211	55	533
40	68,683,109	69,438,084	68,683,109	203	49	461
40	68,683,109	69,840,373	68,780,011	202	53	504
40	68,683,109	69,727,906	68,860,675	202	53	503
40	68,683,109	68,792,808	69,588,458	203	45	374
40	68,683,109	69,935,585	69,099,361	202	45	641
40	68,683,109	69,621,046	68,683,109	205	54	733
40	68,683,109	69,817,395	73,987,050	204	54	261
40	68,683,109	69,686,863	68,938,338	205	54	508
40	68,683,109	70,462,463	71,391,926	204	45	371

TABLE A3 Full results of the three cable layout optimisation methods for the hypothetical test cases of 61 and 122 turbines

No. turbines	Objective value (£) (Optimality ratio)			Comp. time (s)		
	MILP	ACO	ACOsp	MILP	ACO	ACOsp
61	103,255,681	108,888,532	104,495,408	1001	166	918
61	103,255,681	109,304,565	105,255,466	946	168	1531
61	103,255,681	107,852,746	104,171,024	948	169	1454
61	103,255,681	109,067,619	104,156,885	949	169	2056
61	103,255,681	108,366,035	104,939,532	950	166	1264
61	103,255,681	107,900,829	105,021,094	943	148	1379
61	103,255,681	111,998,888	105,113,423	943	156	773
61	103,255,681	111,298,981	104,874,937	948	173	1660
61	103,255,681	125,194,485	104,634,856	942	158	1909
61	103,255,681	107,796,489	103,856,300	941	164	2226
122	<i>197,401,005</i>	211,786,176	198,257,682	<i>16850</i>	843	12024
122	<i>197,401,005</i>	211,201,872	198,321,383	<i>12280</i>	849	11400
122	<i>197,401,005</i>	211,399,235	200,539,889	<i>12249</i>	865	10012
122	<i>197,401,005</i>	212,635,115	200,543,388	<i>12319</i>	773	7077
122	<i>197,401,005</i>	209,805,860	198,410,360	<i>12391</i>	846	11103
122	<i>197,401,005</i>	222,826,513	201,505,632	<i>14781</i>	822	9261
122	<i>197,401,005</i>	210,545,252	198,037,874	<i>13303</i>	826	9856
122	<i>197,401,005</i>	211,575,736	198,195,071	<i>13159</i>	865	12906
122	<i>197,401,005</i>	209,910,343	199,846,143	<i>13201</i>	833	9126
122	<i>197,401,005</i>	211,713,753	199,358,479	<i>16639</i>	804	7149

(Results in italics indicate an unfinished result).

TABLE A4 Full results of the three optimisation methods for the hypothetical test case of 25 turbines, including the cable crossing constraint

No. turbines	Objective value (£) (Optimality ratio)			Comp. time (s)		
	MILP	ACO	ACOsp	MILP	ACO	ACOsp
25	50,268,994	52,871,395	50,358,286	79	31	232
25	50,268,994	51,476,879	50,664,055	79	32	169
25	50,268,994	51,444,607	52,079,903	78	31	202
25	50,268,994	51,194,029	50,664,055	78	31	306
25	50,268,994	51,287,461	50,662,610	78	30	180
25	50,268,994	50,638,853	52,128,744	78	30	286
25	50,268,994	51,082,109	50,638,853	78	30	465
25	50,268,994	50,760,320	50,319,503	78	30	163
25	50,268,994	50,664,055	50,465,140	79	30	212
25	50,268,994	51,656,498	50,288,389	79	30	219